 Philips Res. Rep. 8, 343-366, 1953

STUDIES ON MAGNETIC RECORDING *)

by W. K. WESTMIJZE 621.395.625.3

V. COMPARISON WITH EXPERIMENTS

1. Experimental arrangement

Having discussed in the preceding parts the macroscopic behaviour of the magnetic tape in a homogeneous field, the influence of the gap on recording and reproduction, and the magnetic behaviour of a sinusoidally magnetized tape under the influence of the demagnetizing field, we shall now compare the results of these calculations with the observed relation between input and output voltages.

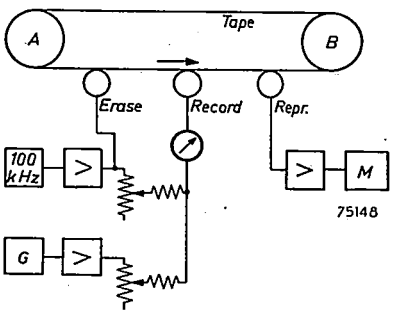

Fig.29. Schematic diagram of experimental arrangement.

A schematic diagram of the arrangement used in the experiments is given in fig. 29. An endless loop of tape is transported with constant speed in the indicated direction over the rollers A and B. Thus an element of the tape has to pass successively the erasing, the recording and the reproducing head.

The erasing head is fed by a 100-kHz oscillator and amplifier which delivers a current of sufficient strength to remove any previous recording. From the same generator is derived the biasing current for the recording head. The amplitude of this current may be adjusted with a potentiometer.

A low-frequency generator G supplies an input current of variable amplitude and frequency which is, after suitable amplification, superposed on the biasing current through the recording head. The frequency range covered extends from 50 Hz to 15000 Hz.

*) Continued from Philips Res. Rep. 8, 148-157, 161-183, 245-269, 1953.

The variations of the flux through the coil of the reproducing head due to the passage of the magnetized tape induce in this coil a voltage that is amplified and fed to a voltmeter, a distortion meter, or other measuring device M. For some of the measurements it is useful to insert an integrating network in the amplifier. In this way the rise with frequency of the output voltage is compensated and the resulting voltage is a better measure of the flux in the tape.

Both recording and reproducing head consist of a magnetic circuit with a gap 0·4 mm high, filled with a 6-μ non-magnetic and non-conducting distance piece. The actual gap length, measured under a microscope, varies from 6·5 to 8 μ. The cross-section of the rest of the circuit is such that its reluctance is negligible compared with that of the gap. The core is built up of mu-metal laminations, the thickness of which are 50 μ for the recording and 100 μ for the reproducing head. The number of turns of the coil is 125 for the recording and 350 for the reproducing head.

The tape used for the present experiments was the same as that with which the magnetic measurements of section 3 of Part III were carried out. The width of the tape was $b = 6{\cdot}3$ mm, thickness of the magnetic coating $d = 15$ μ, and relative permeability of the tape $\mu = 3{\cdot}6$.

Distortion measurements were carried out at a frequency of 250 Hz. The fundamental in the integrated output signal was cut off by a 400-Hz high-pass filter and the remaining harmonics amplified and compared with the original signal. Owing to symmetry, only odd harmonics occur in tape measurements, and of these the third is predominant. The ratio of the amplitudes of the third harmonic and the fundamental in the output signal is used as a measure of the distortion.

2. Output versus biasing current

If the biasing current is varied, at a constant signal current of 250 Hz,

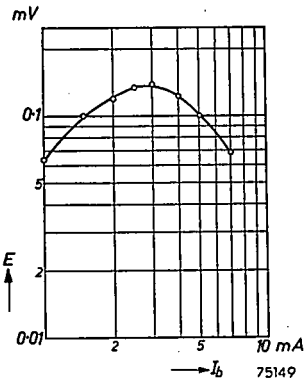

Fig.30. Output voltage as a function of biasing current, at a signal current of 0·2 mA, 250 Hz.

an output curve is obtained (fig. 30) with a maximum at a biasing current of 3 mA. At low frequencies, where the recorded wavelength is long compared with the length of the gap of the reproducing head and with the thickness of the tape it can be assumed that the recorded flux is reproduced without error. For instance at the frequency of 250 Hz and a tape speed of 0·76 m/sec the wavelength is 3 mm. It may be seen in fig. 23*b* that for a tape thickness of 15 μ the influence of the demagnetization in the tape is very small. The gap loss at this frequency is completely negligible. Moreover, at this frequency it can be assumed that the phase of the signal is constant during the time an element of tape passes that region where the recording process takes place.

It should therefore be possible to obtain the variation of the recorded flux with the biasing current from the experiments and calculations of the preceding chapters. A complication here is the variation of the field with the distance at which an element of tape passes the head. The simplest way for the calculation of the flux is to suppose at first that biasing and signal currents are varied proportionally. Then the variation of the recorded magnetization with the depth in the tape can be constructed in the following way.

From fig. 7 can be read the maximum fieldstrength H that is experienced by an element of tape passing the gap at a certain distance y, expressed in the fieldstrength H_0 deep in the gap. This gives, in fig. 31*a*, H/H_0 as a function of y for a gap length of 7 μ, as is the case for the recording head used.

The relation between the remanent magnetization and the maximum values of the biasing and signal fields experienced can be read from fig. 18. For a signal field equaling one tenth of the biasing field this remanent magnetization is given in fig.31*c* as a function of the biasing field. For

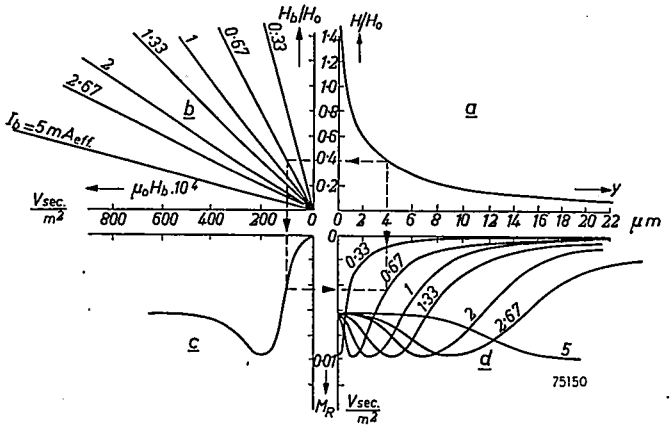

Fig.31. Construction of the recorded magnetization as a function of biasing current and distance to the head. For explanation see text.

reasons of simplicity it is here supposed that the recorded magnetization is longitudinal. The field in the gap is found from $H_0 = nI/l$, where n is the number of turns of the recording coil, I the current through this coil, and l the gap length. Therefore, the biasing field H_b is derived from

$$\mu_0 H_b = \frac{H_b}{H_0} \frac{\mu_0 n I_b}{l},$$

where I_b is the biasing current. Hence the remanent magnetization as a function of y is found by combining figs 31*a* and 31*c* with fig.31*b*, the latter giving $\mu_0 H_b$ as a function of H_b/H_0 for some values of the biasing current. This construction gives the curves of fig.31*d* for different values of the biasing current. The remanent flux in a tape is obtained by integration of M_R over the surface of the tape.

It is seen that for small biasing currents the recorded magnetization has a maximum near the side of the tape nearest the recording head, and therefore the total flux depends to a large amount on the distance between tape and head. For larger values the maximum is shifted to deeper layers of the tape.

In order to obtain the remanent flux as a function of the biasing current for a constant value of the signal current it must be remembered that in fig.31*d* the signal current increases proportionally to the biasing current. Since the signal current is supposed to be very small the recorded magnetization may be taken as proportional to the signal current, which enables us to reduce the curves to one signal-current level.

Carrying out the computation for a tape of 15 μ thickness and 6·2 mm width, and for some values of the space between head and tape, the curves of fig.32 are found for the variation of the recorded flux with the biasing current at a constant signal current of 0·2 mA. In this figure the measured points are also plotted. The flux corresponding to the measured voltage is computed with $\Phi = \frac{E}{2\pi n f}$, where n is the number of turns of the head, and f the measuring frequency; in our case $n = 350$, $f = 250$ Hz.

Qualitatively the agreement between the observed points and the calculated curves is reasonable. The maximum in the measurements, however, occurs at a higher biasing current, while its level is lower.

The deviations between the experimental and the calculated curve may be due to three causes. Firstly, it was assumed in the calculation that the permeability of the tape was unity, while in reality the permeability of the tape was 3·6. The error introduced in this way will be most marked for the layers of the tape close to the head, and will therefore be most pronounced at small currents, where these layers give the main contribution to the recorded flux. Secondly, the direction of the recorded magnetiza-

tion varies over the thickness of the tape and is, moreover, dependent on the amplitude of the biasing current. Thirdly, the direction of the biasing field varies as the tape passes the gap, this variation being especially rapid for the layers of the tape close to the head. It is therefore to be expected that an output reduction will occur at small biasing currents.

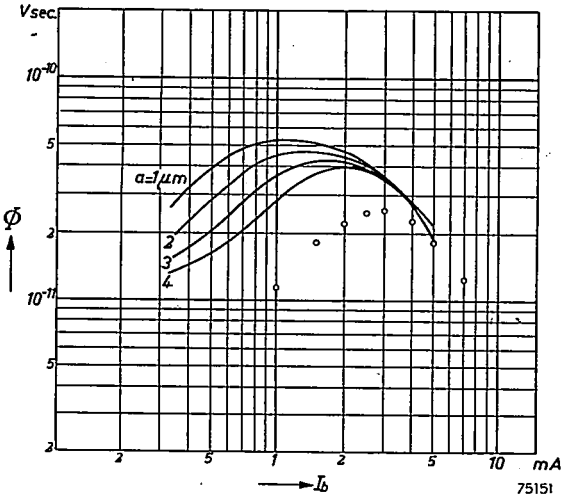

Fig.32. Computed (full curves) and measured flux (circles) as a function of biasing current.

From fig.31*d* it is seen that the decrease of the recorded flux for large values of the biasing current is due mainly to the finite thickness of the magnetic coating of the tape, so that the peak of the curve shifts to values of y beyond the coating. It is therefore understandable that for homogeneous tapes the reduction in the output for high biasing currents is slower and therefore the maximum in the output vs biasing curve is less pronounced than for coated tapes.

3. Distortion

In order to obtain a good reproduction the distortion has to be kept within certain limits. A measure for this distortion may be found in the harmonics generated, if a purely sinusoidal signal is fed to the system. For sound recording it is found that if the harmonic distortion does not exceed 2% it is hardly perceptible.

The dependence of third-harmonic distortion on biasing and signal currents is very complex as may be seen from fig.33, where the ratio (d_3) of third harmonic to fundamental is plotted against the signal current for different values of the biasing current. We shall not attempt here to give a full explanation of the peculiarities of these distortion curves.

However, some features may be explained starting from the measured M-H curves of fig.18.

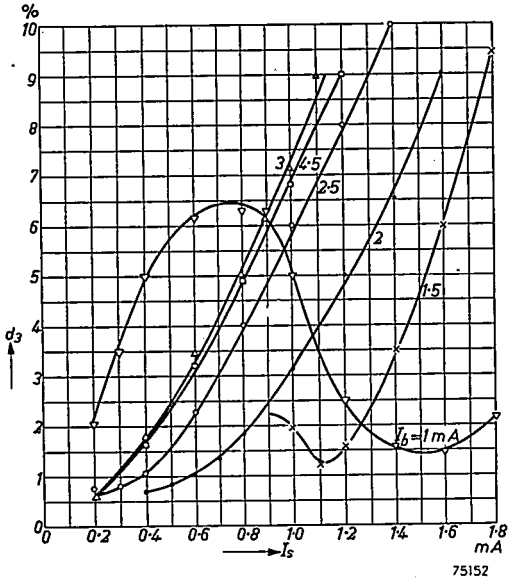

Fig.33. Third-harmonic distortion as a function of signal current for some values of the biasing current.

For small values of the a.c. field (smaller than the coercive force) these curves are convex in the origin, then follow a linear part and next, owing to saturation effects, they become concave with respect to the H-axis. Thus in first approximation they may be described by

$$M = aH + bH^3 - cH^5.$$

The inflexion point of this curve is situated at

$$H = \sqrt{\frac{3}{10}\,\frac{b}{c}}.$$

If now H varies with time according to $H = H_0 \sin\omega t$, it follows that

$$M = (a + \frac{3}{4}b\,H_0^2 - \frac{5}{8}c\,H_0^4)H_0\sin\omega t - (\tfrac{1}{4}b - \frac{5}{16}c\,H_0^2)\,H_0^3\sin 3\omega t -$$

$$- \frac{1}{16}c\,H_0^5\sin 5\omega t.$$

Hence we see that the third harmonic is zero for $H_0 = \sqrt{4b/5c}$, which means that the r.m.s. value of the signal field equals approximately the fieldstrength of the inflexion point.

From fig.18 it is seen that for small biasing fields the inflexion point is found at signal fields of approximately $\mu_0 H \approx 10^{-2}$ Vsec/m^2. Since for small biasing fields a magnetization is recorded close to the head only (cf. fig.31*d*), i.e. where the field is about 4/10 of that in the gap, the minimum of the third harmonic is to be expected in this case for signal currents of approximately 1·4 mA. This is in good agreement with the measured values.

Another feature that is clear from this point of view is that the minimum in the distortion curves is reached for smaller signal fields the higher are the biasing fields, in accordance with the shift to smaller fields of the *M-H* curves (fig. 18) with increasing a.c. fields.

For biasing fields of the order of the coercive force the minimum disappears completely. However, the picture is confused by the fact that the biasing field decreases with the distance from the head, whence there is always a transition layer where distortion occurs. Therefore, the resulting flux in the head is a superposition of the magnetization from layers where the biasing field is too weak, layers where it has just the appropriate strength, and layers where it is too strong and gives a reduction in the output.

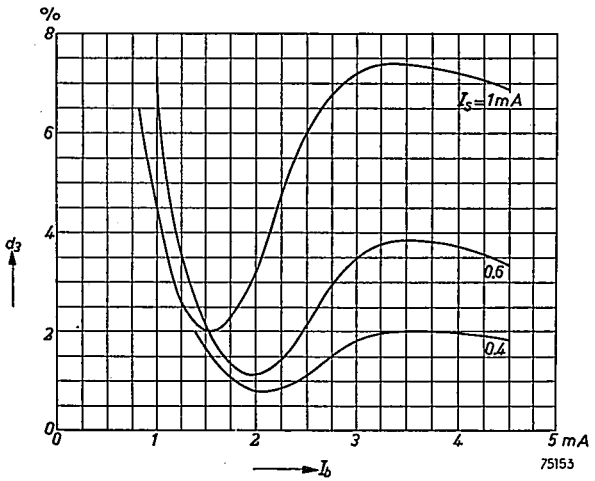

Fig.34. Third-harmonic distortion as a function of biasing current, for some values of the signal current.

Usually the distortion is plotted against the biasing field for constant values of the signal field. These curves (fig.34) can be constructed from fig.33. From what was said above it is clear that the minima of these curves may be partly due to the extinction of a third harmonic generated in the surface layers by a third harmonic of opposite sign generated deeper in the tape. If now the signal frequency is raised and the recorded wave-

length consequently decreased, the demagnetizing effect has more influence on the inner than on the surface layers and thereby the cancelling of the third harmonic is disturbed. This explains why it is sometimes observed that, when at low frequencies the distortion has been brought within reasonable limits by a critical choice of the biasing current, there may still be an appreciable distortion for higher signal frequencies.

4. Frequency characteristic

In the preceding chapters we discussed the output at low frequencies, where the demagnetization and gap loss could be neglected. When the frequency is raised we can assume that the recorded magnetization is at first independent of frequency, i.e. as long as there is no appreciable phase change of the signal field during the passage of an element of the tape past the gap.

The loss due to the finite length of the reproducing gap for a tape of unit permeability can be found from fig.9. For a gap of 7 μ as used in the experiments this gives, even at the shortest wavelength used (13 μ occurring at a tape speed of 19 cm/sec and a frequency of 15 kHz) a

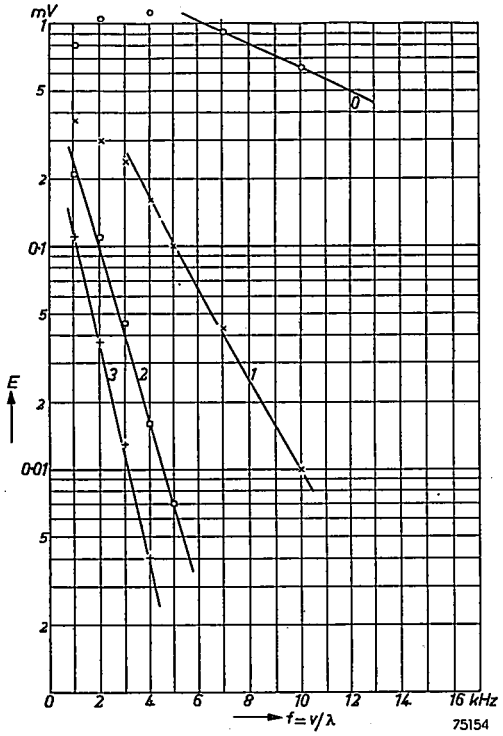

Fig.35. Voltage measured across reproducing coil as a function of frequency with 0, 1, 2 or 3 paper sheets between head and tape.

deviation not exceeding 6 dB. It may be assumed therefore that the application of the correction according to fig.9 will not introduce serious errors in our case where $\mu \approx 4$.

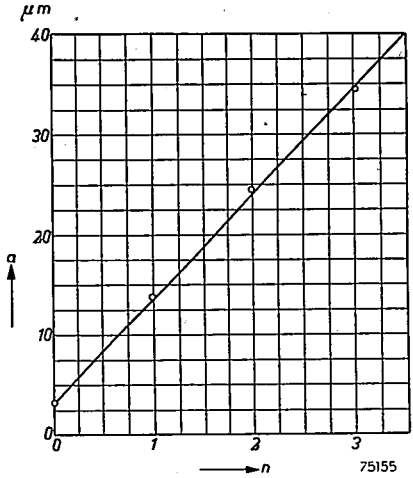

Fig.36. Calculated separation between tape and head against the number of sheets between the two.

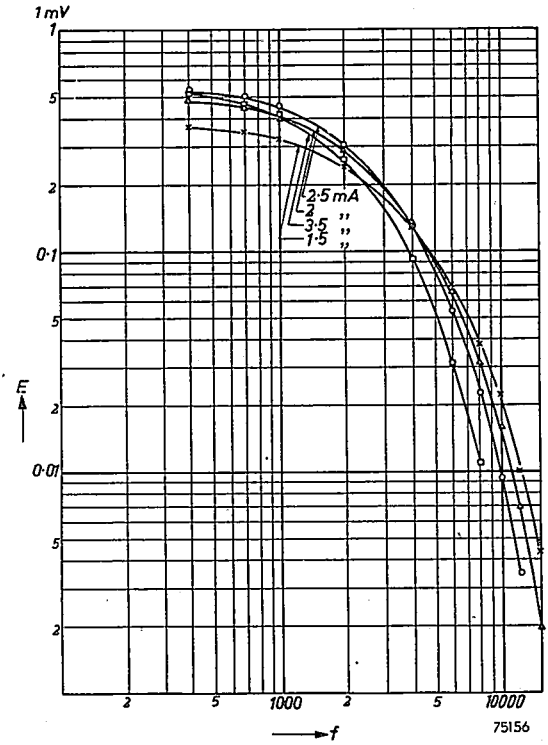

Fig.37. Frequency response for some values of the biasing current.

The reason for the output reduction that remains after this correction has been applied is to be sought mainly in the combined effect of demagnetization and distance to the head as given by eqs(8) and (11) depending on whether the magnetization is longitudinal or perpendicular.

It is seen from eqs (8c) and (11c) that at short wavelength the reproduced flux is

$$\Phi = \Phi_0 \frac{\lambda}{2\pi d} \frac{2}{\mu + 1} e^{-2\pi a/\lambda},$$

while the output voltage is given by

$$E = 2\pi f \Phi = \frac{v}{d} \frac{2}{\mu + 1} e^{-2\pi a/\lambda}.$$

If therefore E is plotted on a logarithmic scale vs $f = v/\lambda$ a straight line is obtained for those frequencies where the approximation holds.

In fig.35 this is done for the case where the same recording is played back with one or more thin sheets of paper (9 μ each) placed between tape and reproducing head. By computing a in the above equations from the slopes of the lines through the measured points we obtained a satisfactory agreement between the calculated spacing and the actual thickness of the sheets (fig.36). It appears that direct contact between head and tape is equivalent to an effective spacing of 3·5 μ.

That the recording process too has a marked influence on the frequency characteristic is shown by fig.37, which represents a measurement of the reproduced flux as a function of the frequency for some values of the biasing current. Some of the peculiarities of these curves are clear from the discussion in section 2. The rise and subsequent fall of the output with biasing current at the low-frequency end of the curves was explained in that section. Where, furthermore, the reproduced flux at the high frequencies is determined mainly by the surface layers it is clear from fig.31*d* that high biasing currents will cause an output loss at these frequencies, since the magnetization of the surface layers is decreased.

Another reason for the output reduction at the high-frequency end may be found in the recording process itself, viz. in the phase change during the recording process already mentioned. This process takes place in a critical range of fieldstrengths round the coercive force. It is therefore important that this range is passed as quickly as possible. If, however, the biasing current is increased, the place where this range is passed is shifted away from the recording gap and is at the same time extended. It will then take an element of tape more time to pass it, and in this way a loss at high frequencies is caused due to the phase change.

Since the change of phase is proportional to the frequency f, and as the time of passing the critical range is inversely proportional to the tape speed v, the determining factor for the loss is the recorded wavelength $\lambda = v/f$.

This effect, which may be called recording demagnetization, was determined in an elegant way by Muckenhirn [31]). He measured the field distribution in front of a 20-μ gap with an 8-μ wire, then calculated the sequence of fields an element of tape was subjected to by the combined action of signal and biasing fields during the passage of the recording gap, and next measured the remanent magnetization when a tape in a homogeneous field was subjected to the same sequence of changes. In this way a loss of 19 dB was found at a wavelength of 25 μ.

In our case a similar experiment might be performed making use of the computed distribution of the field in front of the recording gap. Because of the inhomogeneity of the field owing to the small gap length, however, these computations and measurements would be rather delicate and tedious. It may be estimated that for the smaller gap used in our case the output reduction will be less than in the case of the 20-μ gap used by Muckenhirn.

If now we wish to compare the measured frequency characteristic with the calculations given in Part IV for the case that there is no loss in the recording, we have first to decide whether to use eq.(8) or eq.(11) and we have to insert in these formulae values for the tape thickness d, the spacing a, and the permeability μ.

It is believed that the magnetization, although its direction may vary over the thickness of the tape, is mainly longitudinal because the maximal value of the magnetizing field is longitudinal. We shall therefore use eq.(8) for longitudinal magnetization.

The thickness of the magnetized layer depends on the biasing current. It is seen from fig.31*d* that for a biasing current of 1·5 mA $d = 8$ μ is a reasonable estimate. With a 2·5-mA biasing current, practically the whole coating is magnetized, so that $d = 15$ μ. The permeability may be taken as $\mu = 4$.

Taking for the separation between head and tape $a = 2$ μ it is seen from fig.38 that a good agreement between the experimental and the theoretical curve is obtained for a 1·5-mA biasing current. For the 2·5-mA curve the deviations are greater, especially at the higher frequencies. These deviations may be attributed to the phase change during the recording, which has, as we have seen, more influence at higher biasing currents.

In conclusion we may state that the theoretical considerations of

Parts II, III and IV are sufficient to account for the essential features in the recording process determined experimentally.

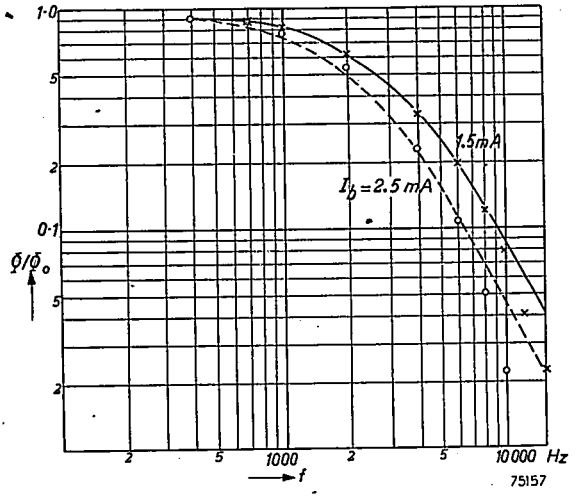

Fig.38. Calculated and measured frequency responses for two values of the biasing current.

In order to obtain an exact quantitative agreement it would be necessary to make more detailed calculations which, however, would require an extremely accurate determination of the geometric configuration and of the magnetic properties of the special tape considered. In our opinion, however, such a very laborious extension of the theory would not reveal any essentially new aspects of the problem. Also the technical value would be extremely limited.

VI. CHANGE IN THE RECORDING WITH TIME

1. Conservation of a magnetic recording

In the preceding parts we have discussed the processes that lead to the recording of information consisting of the variation of a quantity with time as the variation of the magnetic state along the length of a magnetic tape, and the subsequent reproduction whereby the original information is regained as a variation with time. In this part we shall see if the information stored on the tape can be preserved over a period without being subjected to unacceptable changes.

One kind of change that a recording can undergo is that it is attenuated

proportionally to the recorded magnetization. For the recording of sound a certain amount of such a proportional attentuation can be tolerated since a decrease of 10% of the amplitude of a reproduced signal can hardly be heard and a greater decrease can be compensated afterwards by suitable amplification. Even if the higher frequencies would be attenuated more than the lower ones this could be overcome by the use of correcting networks. These corrrections, however, are limited by the background noise since this, too, is amplified.

More serious in the case of sound recording is that extraneous fields may introduce magnetizations that are incoherent with the recorded magnetization. Even if these additional magnetizations are at a very low level they may be very annoying.

These additional magnetizations may be introduced when a tape is stored on a reel, because then the magnetization in one layer of the tape may give rise to a stray magnetization in adjacent layers of the reel. The magnetization effected in a this way is called spurious or accidental printing, or print effect. It may happen that this spurious magnetization extends over several layers on the reel, to the inside as well as to the outside. In playback this is heard as one or more pre- and post-echoes. The former, in particular, may be very disturbing in sound recording.

Of course care should be taken that a recorded reel is not subjected to a field of some strength, for then a partial erasing may take place. Here the accompanying print effect will be far more serious since this field will act as a biasing field superimposed on the field from the adjacent layers.

In the next section we shall investigate, experimentally as well as theoretically, the change of magnetization with time under the influence of weak fields.

2. Print effect

Investigations into the print effect have been carried out by Lippert [32]), Vinzelberg [33]), Johnson [34]), Daniel and Axon [35]) and Wendt [36]). From these investigations it appears that the magnitude of the print effect depends on a number of factors, inter alia, the wavelength of the recorded magnetization, the distance between the layers, the temperature, the time during which the tapes have been in contact and the time elapsed since the ending of the contact. In this section we shall give the observed dependence of the print effect on some of these factors, while in the next section we shall discuss the relation with the magnetic after-effect.

The printing was obtained by bringing part of a loop of a virgin tape for a prescribed time into contact with a magnetized tape in a U-shaped groove made in a piece of metal. In order to rule out as many irreproducible

effects as possible, the contact pressure was kept constant, and the temperature of the metal could be controlled. The loop was then played back in a loop-testing machine. Only sinusoidal signals were used for the measurements.

The amplitude of the printed flux as a function of the amplitude of the magnetizing flux is given in fig.39. Here the flux is plotted on a logarithmic scale along both axes. The slope of the straight line obtained in this way is 1·1, showing that the printed flux is practically proportional to the printing field.

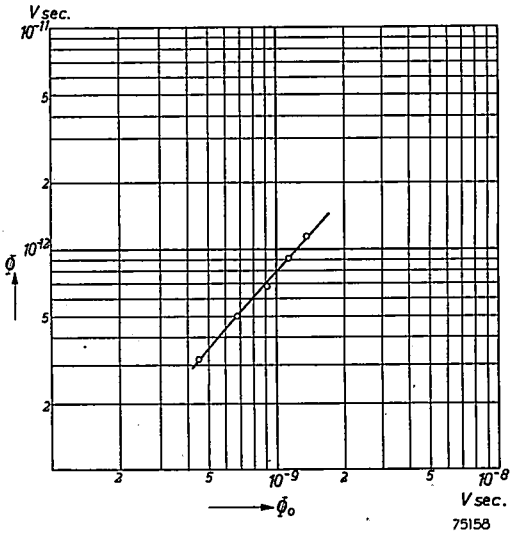

Fig. 39. Amplitude of the printed flux as a function of the amplitude of the flux in the printing tape.

Fig.40 gives the variation of the printed flux Φ with the wavelength λ. Along the abscissa is plotted $v/\lambda = f$, where v is the tape velocity at playback and f the corresponding frequency. It is seen that the printed flux has a maximum at a frequency of 2000 Hz for the tape speed of 762 mm/sec used. This corresponds to a wavelength of 380 μ.

This may be understood in the following way. The field at a distance y from a longitudinally magnetized tape is given by eq.(5c) of Part IV. In this equation we can take $a = \infty$, since no highly permeable metal is present. In first approximation ($\pi d/\lambda \ll 1$) this equation gives for the absolute value of the field:

$$\mu_0 H = B_0 \frac{\pi d}{\lambda} e^{-2\pi y/\lambda}.$$

This shows the general behaviour of the field as a function of the wavelength. At long wavelengths it increases proportionally with $1/\lambda$ because the apparent magnetic poles in the tape increase proportionally with $1/\lambda$.

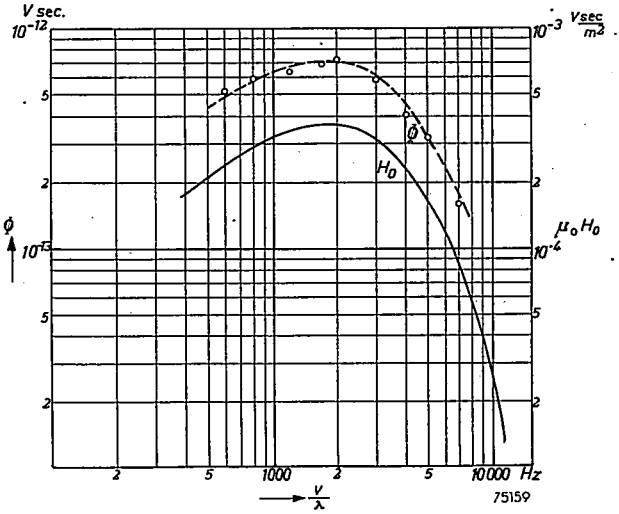

Fig.40. Dependence of printed flux Φ and printing field H_0 on wavelength.

At short wavelengths it decreases exponentially with $1/\lambda$ because of the decrease of the field with the distance from the tape. The maximum value of the field is obtained for $\lambda = 2\pi y$.

If two tapes are brought into contact as is done for the measurement

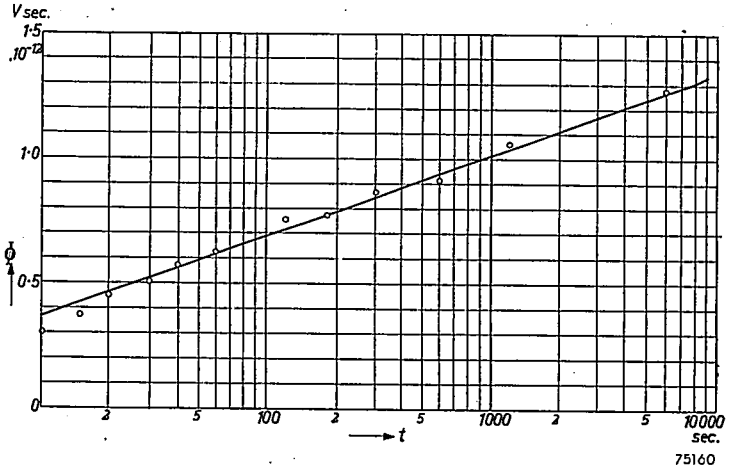

Fig.41. Increase of printed flux with time of contact.

of the print effect we can calculate the amplitude of the printing field with formula (5c) of Part IV, if it is assumed that the permeability of the receiving tape does not affect the field. For a tape with a total thickness $\Delta = 56\ \mu$ and a coating $d = 16\ \mu$, of permeability $\mu = 1{\cdot}7$, as used in the experiments and for an amplitude of the recorded flux $\Phi_0 = 9{\cdot}9.10^{-9}$ Vsec this yields the full-drawn curve of fig.40, representing the printing field H_0 as a function of frequency. The dashed curve of this figure is a shift of the field curve. The close agreement with the measured points shows once more the proportionality of the printed flux with the magnetizing field.

The change of the printed flux with time is shown in figs 41 and 42. In the first it is plotted against the time t_1 during which the tapes have been in contact, measured at a constant time $t_2 = 1$ min after the ending

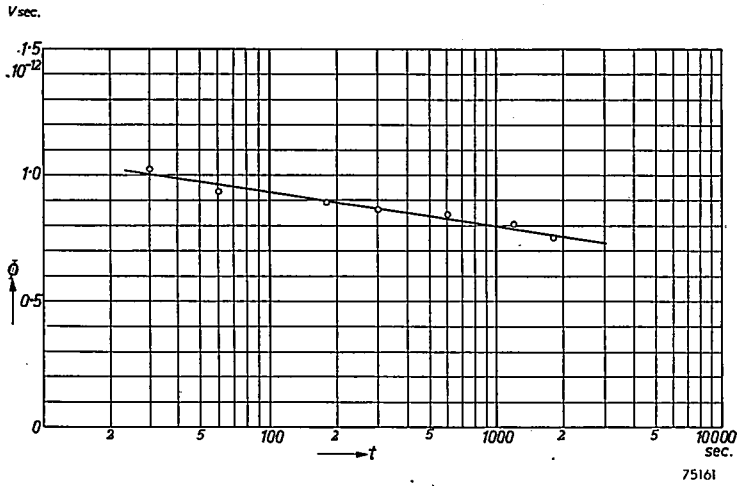

Fig.42. Decrease of printed flux with time after the ending of contact.

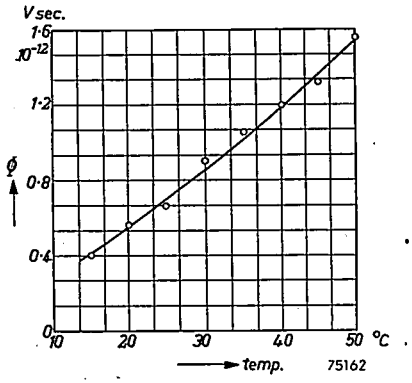

Fig.43. Variation of printed flux with temperature.

of the contact. If the flux is plotted on a linear and the time on a logarithmic scale a straight line is obtained obeying the equation

$$\Phi = 0{\cdot}14.10^{-12} \ln t_1 \text{ Vsec.}$$

Fig. 42 shows the change in the printed flux with the time t_2 since the ending of the contact between the tapes, after a contacting time $t_1 = 10$ min. Here again, an approximately linear relation is obtained, given in this instance by

$$\Phi = (1{\cdot}21 - 0{\cdot}061 \ln t_2).10^{-12} \text{ Vsec.}$$

In both cases the temperature during and after the printing was 30 °C. The dependence on the temperature is given by fig.43, for $t_1 = 10$ min and $t_2 = 1$ min.

The outcome of these measurements will be discussed below.

3. Magnetic lag

If the fieldstrength in a magnetizable medium is changed suddenly, part of the magnetization will, in general, not follow instantaneously but with a certain time lag. A consequence of this lag is that energy losses will occur in an alternating field.

From the measurements made by Preisach [37]) it appearst hat a difference has to be made between a lag for which the principle of superposition does hold, and a lag for which it does not. Néel [38]) distinguishes the two as "trainage reversible" and "trainage irreversible". The first is found for only a limited number of substances in a limited range of temperatures, and the magnetization reaches a definite limit. Snoek [39]) has found that the reason for this lag has to be sought in a relocation of carbon and nitrogen atoms in the crystal lattice.

The second type of lag is found with all ferromagnetic materials. Here the magnetization does not reach a limit but keeps on increasing with ln*t*. Already Preisach mentions as a possible explanation the influence of the Brownian motion on delayed Barkhausen jumps. This idea has been worked out in more detail by Street and Woolley [40]) and by Néel [41])[42]).

Physically, the difference between diffusion lag and fluctuation lag may be seen as follows. The moment after a change of the magnetic field, the Bloch wall between two domains reaches a position of minimal potential energy (*A* in fig. 44). In the case of diffusion lag the strain in the wall will induce some atoms to take other positions in the lattice. In this way the potential minimum is displaced somewhat, e.g. to *B* in fig. 44*a*. If the field is removed the potential hole will after a certain time regain its original position. In the case of fluctuation lag the minimum at *A* is separated by a potential barrier at *C* from a deeper minimum at *B* (fig.44*b*). By

exchange with the lattice the energy of the wall will fluctuate and at a certain time be sufficient to cause the wall to cross the potential barrier.

From the measurements in the preceding section it is seen that the print effect does not approach a certain limit, and we will therefore assume that the print effect can be ascribed to the fluctuation lag.

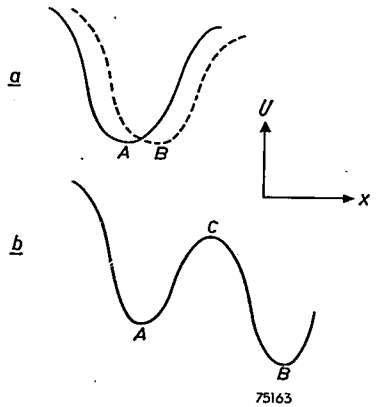

Fig.44. Potential distribution in the case of diffusion lag (*a*) and fluctuation lag (*b*).

The physical picture we can form is as follows. In a magnetic particle the wall separating two domains of different direction of magnetization has a number of preferred positions separated from each other by potential barriers. By interaction with the lattice the wall will occasionally have sufficient energy to cross a potential barrier. In this way an equilibrium position will finally be attained if a large number of walls is present. However, for a position separated by a high potential barrier from a position with lower energy the chance of crossing will be very small, although the latter position has the highest probability. The attainment of the equilibrium state can be accelerated by a rise in temperature, which gives the wall more energy to cross the potential barrier, or by the superposition of an a.c. field as is the case in the ideal magnetization. In this case the height of the potential barrier oscillates so that at a constant energy of the wall the chance of escape is increased.

If now a direct field is applied, the potential energy of the wall is increased proportionally to its displacement. The result is that a redistribution of the walls over the potential holes will take place as a kind of diffusion process. This redistribution is accompanied by an increase of the magnetization in the direction of the applied field. In this picture the permeability must be seen as a reversible displacement of the walls in the potential holes, effecting an increase of the mean magnetic moment

in the direction of the field. If after a certain time the field is removed a permanent magnetization will have been obtained that will be attenuated again by an analogous diffusion process, having as a final result the original distribution.

With this picture in mind we shall try to give an explanation of the print effect. It is also possible to give a discussion for the case where the magnetization is obtained for instance by the rotation of the magnetization of single particles in a cluster. The mathematical treatment will be the same for this case as for the picture discussed here.

We shall here first follow the treatment of Kramers [43]) of the Brownian motion in a field of force.

Le x be the coordinate describing the location of the Bloch wall between two domains, and $U(x)$ the potential of the wall. The equation of motion is

$$m\ddot{x} + r\dot{x} = K(x) + X(t),$$

where m is the apparent mass of the wall, r the damping, $K(x) = -\partial U/\partial x$, and $X(t)$ a term describing the influence of the fluctuations. The existence of the apparent mass of a Bloch wall is due to the moment of inertia of the spins that rotate while a wall is displaced. The magnitude of this mass was calculated by Döring [44]) and Becker [45]).

In the case where the damping r is such that K does not change appreciably over a distance $\sqrt{mkT/r}$, Kramers deduces the equation of diffusion

$$\frac{\partial \sigma}{\partial t} = -\frac{\partial}{\partial x}\left(\frac{K\sigma}{r} - \frac{kT}{r}\frac{\partial \sigma}{\partial x}\right),$$

where $\sigma(x, t)\mathrm{d}x$ is the fraction of an ensemble of equal walls that has at a time t a coordinate between x and $x + \mathrm{d}x$.

In the stationary case this gives a diffusion current

$$w = \frac{K\sigma}{r} - \frac{kT}{r}\frac{\partial \sigma}{\partial x} = -\frac{kT}{r}e^{-U/kT}\frac{\partial}{\partial x}(\sigma e^{U/kT}).$$

Let us now consider a potential function as illustrated in fig.45. Since the diffusion current w is constant between A and B, integration of the equation

$$we^{U/kT} = -\frac{kT}{r}\frac{\partial}{\partial x}(\sigma e^{U/kT})$$

between these points gives

$$w\int_A^B e^{U/kT}\,\mathrm{d}x = \frac{kT}{r}\sigma e^{U/kT}\Big|_B^A.$$

Let the potential at A be represented by $U = \alpha x^2$, and at C by $U = Q - \beta(x-x_A)^2$. Then the integral is found from

$$\int_A^B e^{U/kT}\,dx \approx \int_{-\infty}^{+\infty} e^{Q-\beta(x-x_0)^2/kT}\,dx = \sqrt{\frac{kT}{\beta}}\,e^{Q/kT},$$

and in the case that Q is high enough for a Boltzmann partition to be established, the number of walls in the potential hole at A is found from

$$n_A \approx \int_{-\infty}^{+\infty} \sigma_A e^{-\alpha x^2/kT}\,dx = \sqrt{\frac{kT}{\alpha}}\,\sigma_A.$$

If there are no walls at B, $\sigma e^{U/kT}\Big|_B^A = \sigma_A$, and the number of walls escaping in unit time from A to B is given by

$$W_{AB} = \frac{1}{\tau} e^{-Q/kT} n_A, \text{ where } \tau = \frac{r}{\sqrt{\alpha\beta}}.$$

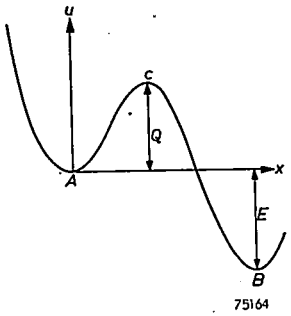

Fig.45. Considered potential distribution.

We shall extend this result of Kramers to the case that walls are also present in the potential hole B. This gives a diffusion current from B to A which must be substracted from the current from A to B. If the potential hole at B has the same shape as that at A, viz. $U = E + \alpha(x-x_B)^2$, then the diffusion current from B and A is given by

$$w_{BA} = \frac{1}{\tau} e^{-(Q+E)/kT} n_B.$$

Let N be the total number of walls divided over A and B then

$$\frac{dn_A}{dt} = w_{BA} - w_{AB} = \frac{1}{\tau}\left\{e^{-(Q+E)/kT}(N-n_A) - e^{-Q/kT} n_A\right\}.$$

This is satisfied by

$$n_A = \frac{N\varepsilon}{1+\varepsilon} + \left(n_0 - \frac{N\varepsilon}{1+\varepsilon}\right) e^{-(1+\varepsilon)qt/\tau},$$

where

$$\varepsilon = e^{-E/kT},$$
$$q = e^{-Q/kT}.$$

If a magnetic field H is applied, E as well as Q will be changed. Let $2\Delta I$ be the increase of the magnetization in the direction of H when a wall jumps from A to B, then the decrease of the energy at x is given by

$$\Delta U = \frac{2\Delta I}{x_B - x_A} Hx.$$

Hence the potential difference between A and B is now $E + 2H\Delta I$, and, if C is midway between A and B the potential difference between C and A is $Q - H\Delta I$.

Had an equilibrium been established before the field was applied, $n_{A0} = N\varepsilon/(1+\varepsilon)$, then at a time t_1 after the application of the field, the number of walls in A would be given by

$$n_{A1} = \frac{N\varepsilon}{e^{2h}+\varepsilon}\left\{1 + \left(\frac{e^{2h}+\varepsilon}{1+\varepsilon} - 1\right) e^{-(1+\varepsilon e^{-2h})\, q e^{h} t_1/\tau}\right\},$$

where $h = \dfrac{H\Delta I}{kT}$.

If at that moment the field is removed the distribution a time t_2 later will be given by

$$n_{A2} = \frac{N\varepsilon}{1+\varepsilon} + \left(n_{A1} - \frac{N\varepsilon}{1+\varepsilon}\right) e^{-(1+\varepsilon)\, q t_2/\tau}.$$

The increase of the magnetization is

$$2\Delta I(n_{A0} - n_{A2}) =$$
$$= 2\Delta I\, N\varepsilon \left(\frac{1}{1+\varepsilon} - \frac{1}{e^{2h}+\varepsilon}\right)\left(1 - e^{-(1+\varepsilon e^{-2h}) q e^{h} t_1/\tau}\right) e^{-(1+\varepsilon) q t_2/\tau}.$$

In reality not all the potential holes will have the same energy difference E, nor all the potential barriers the height Q. Therefore a summation has to be carried out over all E's and Q's. It may be assumed that in the region considered all values of E are of equal probability. When $n(Q)\mathrm{d}E\mathrm{d}Q$ denotes the number of holes with a potential difference between E and $E+\mathrm{d}E$ and a potential barrier between Q and $Q+\mathrm{d}Q$, integration over E gives

$$\mathrm{d}I = 2kT\,\Delta I\, n(Q)\,\mathrm{d}Q \int_0^\infty \left(\frac{1}{1+\varepsilon} - \frac{1}{e^{2h}+\varepsilon}\right)\left(1 - e^{-(1+\varepsilon e^{-2h})qe^h t_1/\tau}\right) e^{-(1+\varepsilon)qt_2/\tau}\,\mathrm{d}\varepsilon.$$

For small values of h the main contribution comes from small values of ε. Hence, neglecting in first approximation ε in the exponent it is found that

$$\mathrm{d}I \approx 4\,kT\,\Delta I\, h\, n(Q)\,\mathrm{d}Q \left\{e^{-qt_2/\tau} - e^{-q(e^h t_1 + t_2)/\tau}\right\}.$$

Integration over Q gives integrals of the type

$$\int_0^\infty n(Q)\, e^{-\varepsilon e^{-Q/kT}}\,\mathrm{d}Q.$$

The function $e^{-e^{-x}}$ is zero for $x \ll 0$, unity for $x \gg 0$, and goes from 0 to 1 in a small interval round $x = 0$. If therefore $f(x)$ is a function that changes little in this interval then

$$\int_0^\infty f(x) e^{-e^{-x+a}}\,\mathrm{d}x \approx \int_a^\infty f(x)\,\mathrm{d}x.$$

Hence

$$I \approx 4(\Delta I)^2 \int_{kT\ln t_2/\tau}^{kT\ln(e^h t_1 + t_2)/\tau} n(Q)\,\mathrm{d}Q. \qquad (1)$$

4. Discussion

The formula deduced above gives the magnetization at a time t_2 after the removal of a field H that has been applied during a time t_1 to an assembly of demagnetized particles. This is exactly what is done in the experiments on the print effect.

The formula shows that the printed magnetization I is proportional to the applied printing field H and to the hatched area in fig.46, representing $n(Q)$ as a function of Q.

The physical interpretation is that for the particles to the left of AB the potential barrier is so low and therefore the time of escape so small that these particles have first crossed the barrier under the influence of the printing field, but have returned already during the time t_2. On the other hand the potential barrier for the particles to the right of CD is so high that the printing time t_1 was not sufficient to effect an appreciable crossing. In the derivation it is assumed that the limits AB and CD are sharp while in reality there is a small region of transition.

It is seen that in the course of time the limit AB is displaced proportional to $kT\ln t_2$ while, if $e^h t_1 > t_2$, the limit CD is displaced proportionally to

$kT\ln t_1$. This explains qualitatively the experimental relation between the print, and t_2 and t_1 respectively. Néel arrives at the same result but along a different line.

That the experimental proportionality constant is higher for the increase with $\ln t_1$ than for the decrease with $\ln t_2$ may be explained if $n(Q)$ increases with Q. This could explain also the rapid increase of the printed magnetization with the temperature.

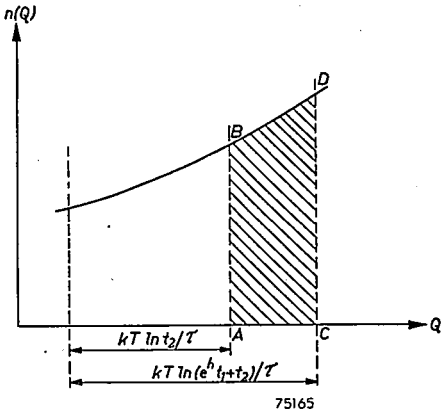

Fig.46. Fictitious distribution of the number of potential barriers over Q. The hatched area shows the barriers that contribute to the print effect.

A certain increase of $n(Q)$ with Q is to be expected. For in the ideal case all the potential barriers should be of equal height Q_0, where Q_0 is such that the barrier is just crossed instantaneously if the coercive field-strength is applied. The function $n(Q)$ is in that case a peak function with a peak at Q_0. In reality the Q's have a certain distribution round Q_0 which means that $n(Q)$ will rise for small Q, fall for high Q, and have a maximum that is reached for field of about coercive strength. For the small printing fields of about 4.10^{-4} Vsec/m^2 we can therefore expect to be in a rising part of the $n(Q)$ versus Q curve.

Eindhoven, March 1953

REFERENCES

[1]) E. Schüller, Elektrotech. Z. **56**, 1219-1221, 1935.
[2]) S. J. Begun, Magnetic Recording, Murray Hill Books, New York, 1949.
[3]) V. Poulsen, Ann. Phys., Lpz. **3**, 754-760, 1900.
[4]) C. Stille, Elektrotech. Z. **51**, 449-451, 1930.
[5]) F. Pfleumer, German patent No. 500900, 31 Jan. 1928.
[6]) V. Poulsen and P. O. Pederson, U. S. Patent 873084, 10 Dec. 1907.
[7]) W. L. Carlson and G. W. Carpenter, U. S. Patent 1640881, 30 Aug. 1927.

[8]) K. Nagai, S. Sasaki, J. Endo, Nippon elect. Commun. Engng 445-447, Nov. 1938.
[9]) Akust. Z. **6**, 264, 1941.
[10]) H. Lübeck, Akust. Z. **2**, 273-295, 1937.
[11]) R. Herr, B. F. Murphy and W. W. Wetzel, J. Soc. Mot. Pict. Engrs **52**, 77-87, 1949.
[12]) R. L. Wallace, Bell Syst. tech. J. **30**, 1145-1173, 1951.
[13]) A. D. Booth, Brit. J. appl. Phys. **3**, 307-308, 1952.
[14]) D. L. Clark and L. L. Merrill, Proc. Inst. Radio Engrs, N.Y. **35**, 1575-1579, 1947.
[15]) G. N. Watson, A treatise on the theory of Bessel functions, Cambridge Univ. Press 1922, p. 180.
[16]) Ibid., table VIII, p. 752.
[17]) S. J. Begun, Audio Engng **32**, 11-13, 39, Dec. 1948.
[18]) P. E. Axon, B.B.C. Quart. **5**, 46-53, 1950.
[19]) O. Schmidbauer, Frequenz **6**, 319-324, 1952.
[20]) A. H. Mankin, Trans. Inst. Radio Engrs PGED-1, 16-21, 1952.
[21]) M. Camras, U. S. Patent 2351004, 13 June 1944.
[22]) H. Toomin and D. Wildfeuer, Proc. Inst. Radio Engrs, N.Y. **32**, 664-668, 1944.
[23]) L. C. Holmes and D. L. Clark, Electronics **18**, 126-136, July 1945.
[24]) W. Steinhaus and E. Gumlich, Verh. dtsch phys. Ges. **17**, 369-384, 1915.
[25]) C. Kittel, Phys. Rev. **73**, 801-811, 1948.
[26]) R. M. Bozorth, Ferromagnetism, v. Nostrand Company, New York 1951, p. 486.
[27]) L. Néel, C. R. Acad. Sci. Paris **224**, 1488-1490, 1947.
[28]) O. Kornei, Electronics **20**, 124-128, Aug. 1947.
[29]) R. Herr, B. F. Murphy and W. W. Wetzel, J. Soc. Mot. Pict. Engrs **52**, 77-87, 1949.
[30]) C. Kittel, Rev. mod. Phys. **21**, 541-583, 1949.
[31]) O. W. Muckenhirn, Proc. Inst. Radio Engrs, N.Y. **39**, 891-897, 1951.
[32]) W. Lippert, Elektrotechnik, Berl. **1**, 56-62, 1947.
[33]) B. Vinzelberg, Funk u. Ton **2**, 633-639, 1948.
[34]) S. W. Johnson, J. Soc. Mot. Pict. Engrs **52**, 619-627, 1949.
[35]) E. D. Daniel and P. E. Axon, B. B. C. Quart. **5**, 241-256, 1950.
[36]) B. Wendt, Veröff. ZentLab. Anilin. photogr. Abt. VII, 314-329, 1951.
[37]) F. Preisach, Z. Phys. **94**, 277-302, 1935.
[38]) L. Néel, J. Phys. Radium **12**, 339-351, 1951.
[39]) J. L. Snoek, Physica, 's-Grav. **6**, 161-170, 1939.
[40]) R. Street and J. C. Woolley, Proc. phys. Soc. Lond. A **62**, 562-572, 1949.
[41]) L. Néel, Ann. Géophys. **5**, 99-136, 1949.
[42]) L. Néel, J. Phys. Radium **11**, 49-61, 1950.
[43]) H. A. Kramers, Physica, 's-Grav. **7**, 284-304, 1940.
[44]) W. Döring, Z. Naturf. **3a**, 373-379, 1948.
[45]) R. Becker, J. Phys. Radium **12**, 332-338, 1951.